Spectral Heterogeneity and Time-Resolved Spectroscopy of Excitation Energy Transfer in Membranes of *Heliobacillus mobilis* at Low Temperatures

Su Lin, Frank A. M. Kleinherenbrink, Hung-Cheng Chiou, and Robert E. Blankenship
Department of Chemistry and Biochemistry, Center for the Study of Early Events in Photosynthesis, Arizona State University, Tempe, Arizona 85287-1604 USA

ABSTRACT Transient absorption difference spectra in the Q_y absorption band from membranes of *Heliobacillus mobilis* were recorded at 140 and 20 K upon 200 fs laser pulse excitation at 590 nm. Excitation transfer from short wavelength absorbing forms of bacteriochlorophyll *g* to long wavelength bacteriochlorophyll *g* occurred within 1–2 ps at both temperatures. In addition, a slower energy transfer process with a time constant of 15 ps was observed at 20 K within the pool of long wavelength-absorbing bacteriochlorophyll *g*. Energy transfer from long wavelength antenna pigments to the primary electron donor P798 was observed, yielding the primary charge-separated state $P798^+A_0^-$. The time constant for this process was 30 ps at 140 K and about 70 ps at 20 K. A decay component with smaller amplitude and a lifetime of up to hundreds of picoseconds was observed that was centered around 814 nm at 20 K. Kinetic simulations using simple lattice models reproduce the observed decay kinetics at 295 and 140 K, but not at 20 K. The kinetics of energy redistribution within the spectrally heterogeneous antenna system at low temperature argue against a simple "funnel" model for the organization of the antenna of *Heliobacillus mobilis* and favor a more random spatial distribution of spectral forms. However, the relatively high rate of energy transfer from long wavelength antenna bacteriochlorophyll *g* to the primary electron donor P798 at low temperature is difficult to explain with either of these models.

INTRODUCTION

Antenna systems of photosynthetic organisms capture incident light energy and transfer excitations to the reaction center, where the energy is stabilized by charge separation. The function of the antenna, therefore, is to increase the absorption cross section per reaction center, ensuring efficient use of incident photons. Many photosynthetic organisms contain antenna complexes that consist of different spectral forms, with the shorter wavelength forms in the more peripheral part of the antenna and the longer wavelength forms in the "core," close to the reaction center. This situation results in a concentration of excitations on the core, increasing the probability of trapping by the reaction center. Another important advantage of spectral diversity of antenna pigments is the more efficient use of photons throughout a large spectral region.

Many species of purple bacteria contain short wavelength-absorbing peripheral antenna complexes (e.g., the B800–850 complex of *Rhodobacter sphaeroides* (Clayton and Clayton, 1972)) and a longer wavelength-absorbing core antenna complex (e.g., B875 of *Rhodobacter sphaeroides* (Van Dorssen et al., 1988; Hunter and Van Grondelle, 1988)). Green filamentous and green sulfur bacteria have large peripheral pigment complexes (up to thousands BChls per reaction center) called chlorosomes absorbing around 740 nm and longer wavelength-absorbing pigments closer to the reaction center (Olson, 1980; Brune et al., 1987; Blankenship et al., 1988). Peripheral pigment complexes are also found in higher plants (LHCI, LHCII) and cyanobacteria (phycobilisomes), with longer wavelength absorbing "core" antenna pigments (Golbeck, 1992).

Besides spectral heterogeneity between peripheral and core complexes, however, considerable spectral heterogeneity is also found within the core antenna of several photosynthetic species. The B875 complex of several species of purple bacteria has been proposed to contain a minor long wavelength component called B896 (Kramer et al., 1984; Van Grondelle et al., 1988), and it has been known for some time that several spectral forms of Chl *a* are present in the core antenna of Photosystem I (Cho and Govindjee, 1970; Owens et al. 1989; Holzwarth et al. 1993; Turconi et al., 1993). Furthermore, the antenna of the recently discovered heliobacteria have been shown to consist of at least three spectral forms of BChl *g* (Van Dorssen et al., 1985; Smit et al., 1989; Trost and Blankenship, 1989). The core antenna pigments of Photosystem I and the antenna of heliobacteria are associated with the reaction center polypeptides, rather than a separate antenna peptide as in purple bacteria, green filamentous bacteria and Photosystem II.

A striking phenomenon of the spectrally heterogeneous core antennae is the apparent presence of pigments that absorb at longer wavelength than the primary electron donor, the ultimate excitation acceptor. This implies that the energy transfer from the antenna to the reaction center is an energetically "uphill" process, which might impair the overall efficiency. It has been suggested that long wavelength pigments are located adjacent to the photoactive pigments and that they would serve to "focus" excitations to the reaction

Received for publication 4 April 1994 and in final form 12 July 1994.

Address reprint requests to Dr. Robert E. Blankenship, Dept. of Chemistry and Biochemistry, Arizona State University, Tempe, AZ 85287-1604. Tel.: 602-965-1439; Fax: 602-965-2747; E-mail: blankenship@asuchm.la.asu.edu.

Abbreviations used: BChl, bacteriochlorophyll; *Hc.*, *Heliobacillus*; RC, reaction center; P798, primary electron donor of heliobacteria absorbing at 798 nm at room temperature; PMS, phenazine methosulfate.

© 1994 by the Biophysical Society

0006-3495/94/12/2479/11 $2.00

center, actually enhancing the efficiency of charge separation (Van Grondelle et al., 1988). However, model calculations have indicated that long wavelength antenna pigments are unlikely to improve the efficiency of trapping by the reaction center (Beauregard et al., 1991). An alternative function of the long wavelength pigments has been proposed by Trissl (1993), who showed that they might actually enhance the efficiency of photon absorption in the long wavelength spectral region, without impairing energy transfer to the reaction center, at least at room temperature. In general, understanding of the organization of spectrally heterogeneous core antenna and the role of long wavelength pigments appears to be far from complete.

The long wavelength component B896 in the core antenna of purple bacteria was initially proposed to serve as a trapping mechanism of excitations close to the reaction center (Van Grondelle et al., 1988). Recently, however, a number of studies have indicated a more random distribution of spectral forms in the core antenna of purple bacteria (Van Mourik et al., 1993).

The long wavelength antenna pigments of the Photosystem I antenna (absorbing at wavelength longer than 700 nm) are still a matter of considerable interest. Their presence has clearly been demonstrated at room temperature (Wittmershaus et al., 1992; Woolf et al., 1994; Hastings et al., 1994), but evidence about their position in the antenna is still scarce. Simulations by Jia et al. (1992) have shown that a "funnel" model (with longer wavelength pigments located close to the reaction center) can be ruled out and that a model in which all spectral forms are randomly distributed in the antenna with one or two long wavelength pigments close to the photoactive pigments of the reaction center best describes the fluorescence kinetics at low temperature. Model simulations by Trinkunas and Holzwarth (1994) also draw a similar conclusion, but their model has the long wavelength-absorbing pigments collected to a cluster and located close to the photoactive pigments, but not in direct contact.

The anoxygenic heliobacteria contain a single pigment-protein complex that serves as a combined antenna and reaction center and is fully contained in the cell membrane. No peripheral antenna complexes are present. About 35 BChl *g* molecules are present per primary electron donor P798 (Nuijs et al., 1985; Trost and Blankenship, 1989; Vos et al., 1989; Van de Meent et al., 1990). Low temperature absorption spectra of *Heliobacterium chlorum* clearly show the presence of at least three spectral forms of BChl *g*, called BChl *g*-778, BChl *g*-793, and BChl *g*-808 after their respective absorption maxima (Smit et al., 1985). Transient absorption measurements indicated that excitations localize mainly on the two long wavelength forms within 1–2 ps at room temperature, after which trapping of excitations by the reaction center occurs in 20–30 ps (Van Noort et al., 1992; Lin et al., 1994). At low temperature, fast excitation transfer to BChl *g*-808 occurred, and long-lived excited states were observed on pigments absorbing around 812–814 nm (Van Kan et al., 1990, Van Noort et al., 1994). Additional evidence for considerable spectral heterogeneity within the BChl *g*-808 pool came from time-resolved fluorescence measurements at 25 K (Kleinherenbrink et al., 1993), which showed several lifetimes and spectral forms. Triplets were found to form (presumably through intersystem crossing from the singlet excited state) on the various long wavelength antenna forms (Kleinherenbrink et al., 1991). Despite the apparent "uphill" energy transfer step from the long wavelength antenna to the primary electron donor in the reaction center, the yield of photochemistry upon excitation of the antenna was still considerable at low temperature (Van Dorssen et al., 1985; Smit et al., 1985; Kleinherenbrink et al., 1992). However, formation of the charge-separated state has not been time-resolved so far under these conditions.

In this paper, we describe transient absorption measurements on membranes of *Hc. mobilis* at 140 and 20 K with sub-picosecond time resolution. We show that energy is transferred to the long wavelength-absorbing pool of antenna pigments within about 1 ps, whereas energy transfer among long wavelength pigments occurs with a much slower time constant of about 15 ps at 20 K. Energy transfer from the long wavelength BChl *g* to the reaction center results in charge separation even at low temperatures. The time constant for this process was found to be surprisingly weakly temperature-dependent. Our results suggest that antenna molecules of different spectral forms are spatially distributed within the antenna system, rather than organized as a funnel with the longest wavelength-absorbing pigments nearest the photoactive pigments.

MATERIALS AND METHODS

Preparation procedures of *Hc. mobilis* membrane fragments and the setup for transient absorption measurements were the same as described by Lin et al. (1994). Samples were suspended in a buffer containing 25 mM Tris (pH 8), 20 mM sodium ascorbate, and 100 μM phenazine methosulfate (PMS). 66% (v/v) of glycerol was added to the sample for 140 K measurements, and 30% of potassium glycerophosphate (PGP) and 60% of glycerol were added to the sample for 20 K measurements to form clear glasses at low temperature. Samples were contained in a low temperature cell with an optical pathlength of 1.2 mm. The typical optical density of the sample in the measuring cell was 1–1.5 at 788 nm at room temperature. The cell was attached to the cooled finger of an Air Products closed circulated helium refrigerator to cool the sample to the desired temperature.

Samples were excited at 590 nm, close to the Q_x transition band of antenna BChl *g*. The laser pulses used were 200 fs full width at half-maximum at a repetition rate of 540 Hz. Transient absorbance changes were measured at the magic angle with respect to the excitation polarization. Excitation intensities were varied using neutral density filters. For low intensity measurements, in which excitation annihilation processes could be neglected, the excitation intensity was kept as low as 1.8×10^{14} photon pulse^{-1} cm^{-2}, corresponding to 0.25 photon pulse^{-1} absorbed per reaction center (Lin et al., 1994).

A concern in low temperature measurements where the sample cannot be flowed is that repetitive flash excitation will lead to a buildup of a large fraction of closed reaction centers. The fraction of closed reaction centers was estimated using the interval between excitation pulses in our laser system, 1.85 ms, and the observed recovery of the ground state at low temperature, 2.3 ms (Smit et al., 1985). For a single exponential decay with this time constant and all of the centers excited and undergoing photochemistry with each laser pulse, 45% of the centers will be closed before the next laser flash. If the laser excitation is lowered so that the fraction of reaction centers excited is 0.25, then only 11% of the centers are still closed at the time of

the next flash. These represent upper limits of the amount of closed reaction centers, because at low temperatures not all excitations lead to charge separation (Kleinherenbrink et al., 1992).

RESULTS

Fig. 1 shows time-resolved absorption difference spectra in the Q_y region from membranes of *Hc. mobilis* at 140 K. For each excitation laser flash, less than 0.25 photons were absorbed per reaction center. The initial spectra show two major bleaching bands at 792 and 808 nm (Fig. 1 *a*). The 792 nm band shows a prompt rise, whereas the 808 nm band was fully developed after about 2 ps. Fig. 1 *b* shows the spectra taken at later times. The 808 nm band shows a slight shift to 810 nm and has disappeared after 100 ps, whereas a bleaching band remains around 792 nm after this time delay.

Transient absorption difference spectra taken on a 150 ps timescale with high and low excitation intensities were fit with a sum of exponentials over the wavelength region from 770 to 830 nm with a 2 nm interval. In the case of low excitation intensity, three kinetic components were adequate to obtain a good fit, with decay-associated spectra shown in Fig. 2 *a*. A positive amplitude in the decay-associated spectrum represents a growing in of the bleaching, and a negative amplitude represents a decay of the bleaching. A component with a time constant of 0.7 ps has negative amplitude below 785 nm and positive amplitude at longer wavelengths. A similar value of this time constant was obtained from a data set with 0.15 ps time resolution (data not shown). This component might contain some contribution from the laser pulse width, but is clearly dominated by the process of excitation energy redistribution, i.e., energy transfer from short wavelength-absorbing BChl *g* to long wavelength-absorbing BChl *g*. The 29.2 ps component has a spectrum peaking at 810 nm and represents the overall excitation decay in the antenna system and the build-up of the charge-separated state. The long-lived component from the fitting is caused by the formation of $P798^+$, showing a bleaching centered around 792 nm.

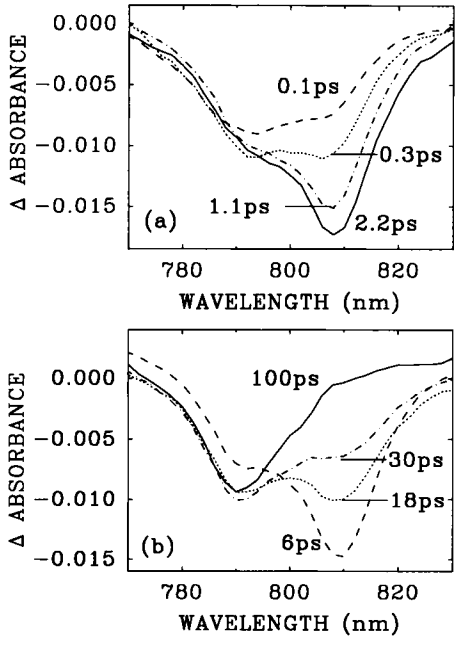

FIGURE 1 Time-resolved absorption difference spectra of membranes of *Hc. mobilis* at (*a*) 0.1, 0.3, 1.1, and 2.2 ps; and (*b*) 6, 18, 30, and 100 ps at 140 K with 590 nm laser excitation with an excitation intensity of which 0.25 photons were absorbed per reaction center. Spectra were taken with a wavelength resolution of 0.14 nm/channel and were averaged over 15 channels to obtain a wavelength resolution of 2 nm.

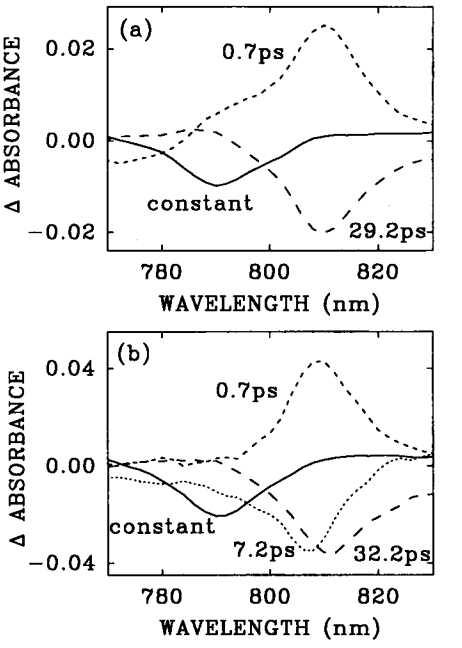

FIGURE 2 Decay associated spectra of membranes of *Hc. mobilis* at 140 K obtained from fitting of transient absorption difference spectra over a 150 ps timescale with a time resolution of 1.5 ps per point (*a*) with low laser excitation intensity of which for each laser pulse 0.25 photon per reaction center was absorbed, and (*b*) with higher laser intensity (about 0.9 photons per laser pulse).

Fig. 2 *b* shows the decay-associated spectra obtained from a data set with higher excitation intensity (about 0.9 photons absorbed per reaction center). Besides the three kinetic components similar to those obtained with low intensity excitation, an additional component with lifetime of 7.2 ps is now obtained. Its spectral profile is very similar to that of the difference spectrum at 2 ps because of antenna bleaching with a slight blue-shift of 1–2 nm (Fig. 1 *a*). We will show in the Discussion that it is reasonable to assign the 7.2 ps component partly to trapping by oxidized P798 but mostly to singlet-singlet annihilation.

Time-resolved spectra of *Hc. mobilis* at 20 K show similar kinetic features as observed at 140 K. Fig. 3 *a* shows the spectra at early times. It can be seen clearly that the majority of the excitations are located on the long wavelength species around 810 nm within 1–2 ps. Difference spectra taken at later times are shown in Fig. 3 *b*. A bleaching around 810 nm decreases with time while a 792 nm bleaching band develops. In addition to the 792 nm band, a bleaching around 814 nm

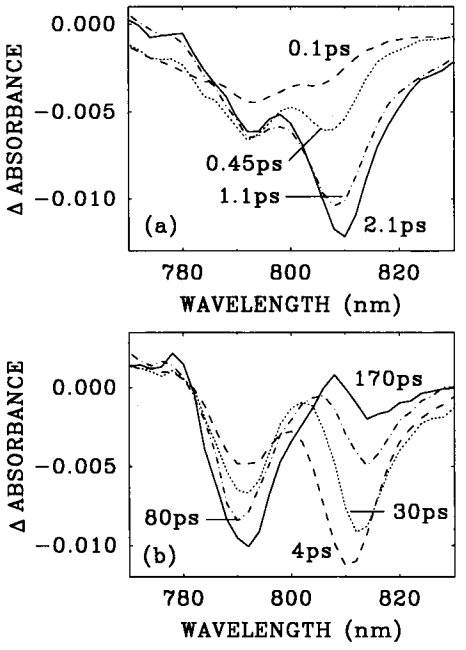

FIGURE 3 Time-resolved absorption difference spectra of membranes of *Hc. mobilis* at (*a*) 0.1, 0.45, 1.1, and 2.1 ps, and (*b*) 4, 30, 80, and 170 ps at 20 K with 590 nm laser excitation with low intensity. Other conditions were the same as in Fig. 1.

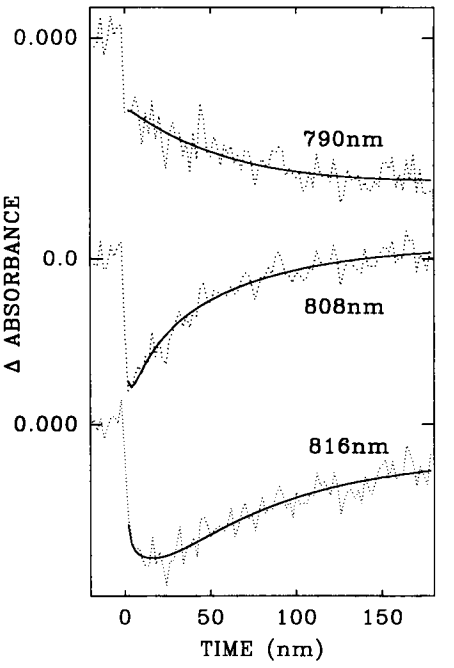

FIGURE 4 Decay profiles at 790 nm (*top*), 808 nm (*middle*), and 816 nm (*bottom*) of membranes of *Hc. mobilis* at 20 K. Solid lines were fits obtained from four component global analysis. Time resolution for the data is 2 ps per point.

remains after 170 ps, most likely because of long-lived excited states on long wavelength-absorbing BChl *g* in the antenna (see Discussion).

Kinetics of absorbance changes at 790, 808, and 816 nm with low excitation intensity at 20 K are plotted in Fig. 4. The smooth curves are fits at corresponding wavelengths obtained from global analysis. At 790 nm, a prompt bleaching is followed by a slower growing in of an additional bleaching. The kinetics at 808 nm show that the recovery of the bleaching is a multi-exponential process. At 816 nm, an instantaneous bleaching is followed by an additional bleaching build-up. The overall decay of the bleaching at this wavelength at later times appears to be slower than that observed at 808 nm.

The four exponential components that were needed to fit the data at 20 K with low excitation intensity (Fig. 4) have decay-associated spectra shown in Fig. 5 *a*. A 1.3 ps energy transfer component shows similar features as the 0.7 ps component observed at 140 K. This component was more accurately determined to be 0.8 ps with a 0.15 ps time resolution measurement (data not shown). The 68.4 ps component has negative amplitude around 811 nm and positive amplitudes over a broad region around 792 nm. Its profile reflects energy transfer from long wavelength antenna BChl *g* to the primary electron donor P798 in the reaction center. The long-lived component has a spectrum that is similar to the spectrum at later times in Fig. 3, which shows bleaching at 792 and 814 nm. Surprisingly, a fourth component with a lifetime of 14.9 ps was clearly needed to fit the data at 20 K. Its spectral shape indicates that it probably reflects energy transfer from shorter wavelength pigments to

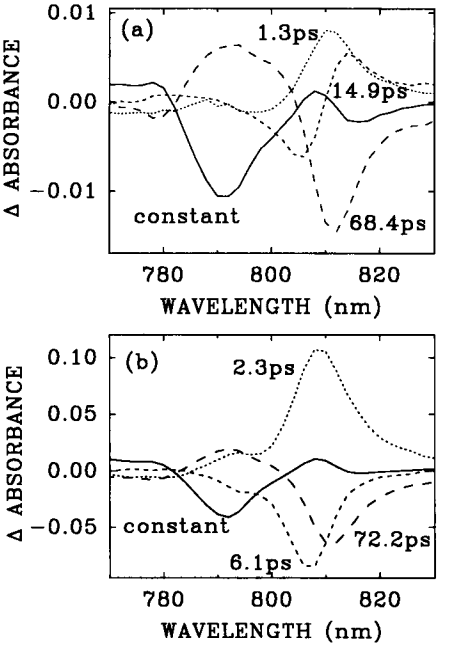

FIGURE 5 Decay associated spectra obtained from global fit of the transient absorption kinetics of membranes of *Hc. mobilis* at 20 K (*a*) with low excitation intensity and (*b*) with high excitation intensity.

longer wavelength pigments within the long wavelength BChl *g* 808 band. The relatively long time constant that characterizes this process suggests that the different spectral forms of BChl *g* are randomly distributed within the antenna and do not form an excitation "funnel" toward the reaction center (see Discussion).

Global analysis of data with higher excitation intensity at 20 K (Fig. 5 *b*) yields a component with a time constant of 6.1 ps, with a spectral profile similar to the 7.2 ps observed at 140 K (Fig. 2 *b*). As with low intensity excitation (Fig. 5 *a*), components with time constants of about 2 and 70 ps and an irreversible component are still observed. However, the 15 ps energy transfer component within the long wavelength antenna pool was not resolved under these conditions.

Transient absorption spectra measured at 295 K (Lin et al., 1994), 140 K, and 20 K show that the excitation energy distribution among different antenna forms changes dramatically with temperature. However, the observed kinetics of excitation transfer and trapping exhibit only a moderate change, especially in the temperature range of 295–140 K. Energy transfer from antenna molecules to the primary electron donor P798 at 20 K was directly observed and still occurred with a fairly high efficiency. Multiphasic energy transfer kinetics among the antenna spectral forms was observed at 20 K, reflecting a complicated energy transfer process within the spectrally heterogeneous antenna system. The kinetic simulations described in the next section give some insights into the pigment organization in the heliobacterial antenna reaction center complex.

KINETIC SIMULATIONS

Model assumptions

A model simulation was done to extract more detailed information about energy transfer and charge separation processes and the possible organization of the antenna within heliobacteria. The numerical simulation was carried out based on a two-dimensional array model of the antenna/reaction center system. In the model, 36 BChl *g* molecules were used to construct a 6 by 6 regular lattice array and a trap (the reaction center) is placed at the center of the array. Each molecule is assigned to a spectral form. The number of molecules in each spectral form, i.e., BChl *g* 778, BChl *g* 793, and BChl *g* 808, was estimated from the Gaussian fitting of the absorption spectrum measured at 5 K by Smit et al. (1985). To represent more accurately the inhomogeneous nature of the antenna, the spectral forms were further divided into three subpools in such a way that the sum of the absorption spectrum of molecules matched the absorption spectrum measured at 5 K (Smit et al., 1985). The numbers of molecules in each spectral form are listed in Table 1. It was assumed that an excitation starting from a given site can be transferred to its four nearest neighboring sites with a microscopic transfer time from higher to lower energy molecules of τ_{ss}. The back transfer rate is governed by the Boltzmann factor, i.e., the back transfer time τ_{back}:

$$\tau_{back} = \tau_{ss}\exp(\Delta E/kT). \quad (1)$$

In Eq. 1, ΔE denotes the energy difference of the two molecules (by convention taken to be positive, as this is an uphill process), k is the Boltzmann constant, and T is the absolute temperature of the system. Transfers to the four next-nearest neighbors were also included in the calculation. Inclusion of these components has little effect on the simulations at room temperature, but it makes a significant difference at low temperature, where excitations tend to get "stuck" in isolated low energy pigments. Because the distance between the next-nearest neighbors is $\sqrt{2}$ longer than that between the nearest neighbors, according to the definition of Förster transfer rate (the rate is proportional to the $1/R^6$) (Förster, 1965), a factor of eight increase of the τ_{ss} was used for the time constant for next-nearest neighbor transfer. The natural decay lifetime is defined as τ_0, which was assumed to be 2 ns. The single step transfer time from four nearest neighbors to the trap is defined as τ_{trap} and the charge separation time constant is defined as τ_{cs}. Nonselective excitation was considered in the calculation in which an excitation starts with an equal probability from all antenna molecules. The probability $P(t)$ of an excitation on each spectral form was calculated as a function of time using Eq. 2:

$$P(t + dt) = P(t) + dP(t), \quad (2)$$

with

$$dP(t) = \sum_i P_i(t)\tau_i^{-1}dt - P(t)\sum_i(\tau_i^{-1})dt - P(t)\tau_0^{-1}dt. \quad (3)$$

In Eq. 3 the summation is over the 4 nearest and 4 next-nearest neighbors i, with τ_i being either τ_{ss} or τ_{back}, depending on the energy difference. The time step dt was 10 fs. The reaction center pigment was treated as an antenna pigment with four nearest neighbors and no next nearest neighbors in the center of the lattice with probability $P_{rc}(t)$ of being excited. The probability of charge separation $P_{cs}(t)$ was calculated using Eq. 4:

$$P_{cs}(t + dt) = P_{cs}(t) + dP_{cs}(t), \quad (4)$$

with

$$dP_{cs}(t) = P_{rc}(t)\tau_{cs}^{-1}dt, \quad (5)$$

where τ_{cs} is the charge separation time.

Two types of antenna arrangement were considered in the simulation. In one case, a funnel model in which antenna molecules are arranged in such a way that the shorter wavelength-absorbing pigments are further away from the trap and the longer wavelength absorbing pigments are close to the trap. The excitation energy is therefore "funneled" to the trap by efficient downhill transfer. In the other arrangement, called the "random" model, antenna molecules representing different spectral forms are randomly distributed. In the random model calculation, the resulting kinetics varies

TABLE 1 Spectral forms (represented by a single wavelength) and number of BChl *g* molecules of each spectral type

λ (nm)	773	778	783	788	793	798	803	808	813
# BChl *g*	4	4	5	5	6	5	1	5	1

with the particular arrangement of the antenna pigments. Therefore, calculated kinetics from 50 different randomly generated configurations were averaged for each given parameter set. Such an average does not necessarily provide the most realistic antenna arrangement. Because detailed knowledge about the antenna structure is lacking, the average of results from different configurations provides a reproducible result for a given set of parameters for the purpose of comparison. However, our results described below should not be taken to indicate that the arrangement of the pigments in the reaction center is different from one complex to the next. In keeping with the results of structural studies of other pigment-protein complexes, we anticipate that the pigment arrangement is probably very similar in each center, but is not such that the energies of the pigments monotonically decrease as they become closer to the trap.

Additional simulations were carried out with both the funnel and random models, in which the trap was moved from the center of the lattice to be near one edge. These simulations produced results very similar to the results described below, in which the trap is assumed to be at the center of the lattice.

Funnel model simulation

Results obtained from the funnel model simulation are shown in Fig. 6. Kinetic traces of antenna and $P798^+$ at 295, 140, and 20 K are shown in Fig. 6, *a*, *c*, and *e*, respectively. Kinetics of the antenna from different spectral forms are combined into two groups; one is at the shorter wavelength side of the trap P798 (773–793 nm), and the other is at the longer wavelength side (798–813 nm). To compare the observed absorbance change within the long wavelength absorbing band BChl *g*-808, individual kinetic traces 803, 808, and 813 nm are plotted in Fig. 6, *b*, *d*, and *f*.

Parameters used in the calculation at each temperature are listed in Table 2. At room temperature, τ_{ss} and τ_{cs} were chosen originally from the estimated time constant from the early work (Lin et al., 1994) and varied in a range of ± 0.1 ps so that the calculated kinetics match the experimental results. It was found that, with τ_{ss} in the range of 0.2–0.25 ps and τ_{cs}, about 0.9–1.0 ps, reasonable kinetics were obtained (see below). τ_{ss} was kept the same at 140 and at 20 K, and the back transfer time constant τ_{back} changed with temperature as shown in Eq. 1. A shorter charge separation time was used at lower temperatures (0.6 ps), assuming that the temperature dependence of τ_{cs} is similar to that of in purple bacteria (Kirmaier and Holten, 1990).

At 295 K, the calculated results (Fig. 6 *a*) show that a fast energy transfer from short wavelength antenna (773–793 nm) to longer wavelength antenna (798–813 nm) occurs within about 1 ps. Then both pigment groups decay with the same time constant of 30 ps, which is also the time constant of the formation of $P798^+$. The result agrees well with the experimental observations at room temperature.

Similar kinetics were obtained at 140 K, using parameters listed in Table 2, except that the amplitudes of each component changed. As shown in Fig. 6 *c*, most of the excitations are located in the longer wavelength forms of the antenna pigments after the equilibration. This amplitude change corresponds to the spectral shape change observed from the time resolved spectra measured at early times (Fig. 1 *a*). The calculated kinetics at 20 K (Fig. 6 *e*) also show a fast equilibration among antenna spectral forms with a time constant of 2 ps. Most of the excitations are concentrated in the 813 nm spectral form and do not lead to charge separation. This is considered in the Discussion.

The arrangement of a funnel model results in simple decay kinetics in all antenna species after the excitation redistribution which occurred within the first 2 or 3 ps. Kinetics of

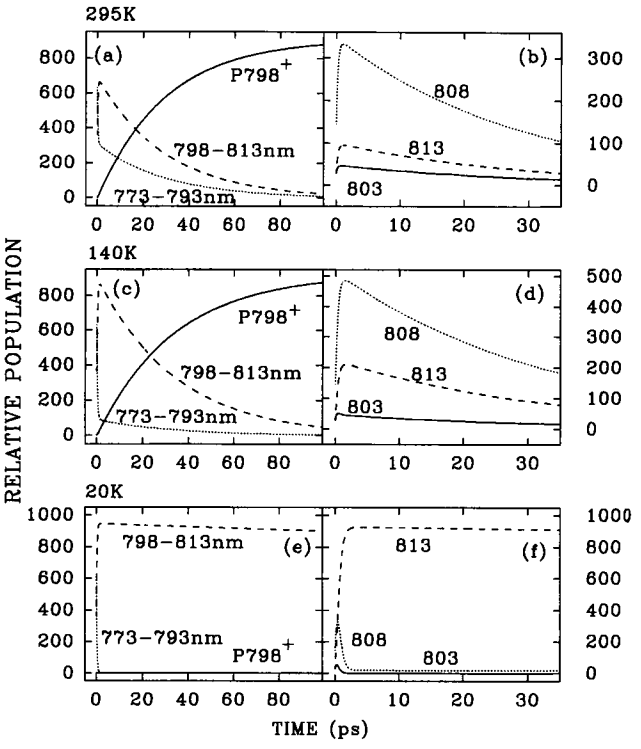

FIGURE 6 Kinetic traces of different antenna spectral forms and $P798^+$ at (*a*, *b*) 295 K, (*c*, *d*) 140 K, and (*e*, *f*) 20 K obtained from model simulation using the funnel model. In *a*, *c*, and *e*, solid lines show relative population of the oxidized $P798^+$, short dashed lines show antenna forms shorter than 798 nm (773–793 nm), long dashed lines show antenna forms longer than 798 nm (798–813 nm). In *b*, *d* and *f*, kinetic traces of the three long wavelength-absorbing species, 803 nm (*solid lines*), 808 nm (*short dashed lines*), and 813 nm (*long dashed lines*).

TABLE 2 Kinetic parameters used in model simulations

Temperature (K)	τ_{ss} (ps)	τ_{trap} (ps)	τ_{cs} (ps)	trap λ (nm)
Funnel model:				
295 K	0.25	0.25	1.0	798
140 K	0.25	0.25	0.6	798
20 K	0.25	0.25	0.6	798
Random model:				
295 K	0.2	0.2	1.0	798
140 K	0.2	0.2	0.6	798
20 K	0.2	0.2	0.6	798

the three longest wavelength species are shown in Fig. 6, *b*, *d*, and *f*. No slower transfer process within the BChl *g* 808 nm band are observed at low temperatures.

Random model simulation

Kinetics simulated using the random model are shown in Fig. 7. Kinetic traces of $P798^+$ and short and long wavelength antenna forms at 295, 140, and 20 K are shown in Fig. 7, *a*, *c*, and *e*, respectively. Results from 295 and 140 K calculations are very similar to that obtained from the funnel model calculation. A fast excitation redistribution takes place in 1 ps and is followed by a 31 ps decay which is caused by the trapping and the formation of the charge-separated state $P798^+$. To obtain the same equilibration and de-excitation time constants as in the funnel model at room temperature, a slightly smaller value for the single step transfer time was used (0.2 vs. 0.25 ps). The low temperature charge separation time, 0.6 ps, was the same as in the funnel model. Kinetics of long wavelength-absorbing species 803, 808, and 813 nm, are shown in Fig. 7, *b*, *d*, and *f*. Besides the fast equilibration occurring within the first picosecond, a slower phase of energy transfer among the antenna spectral forms is also observed. This slow transfer process becomes more pronounced at 20 K. The simulation at 20 K shows a fast excitation redistribution in the long wavelength absorbing pigments followed by a slower transfer to 813 nm pigment.

As in the funnel model, the random model does not adequately simulate the experimental results for the energy trapping to form $P798^+$ at 20 K. However, the random model does reproduce the observed kinetics of energy redistribution among the long wavelength pigments much better than the funnel model.

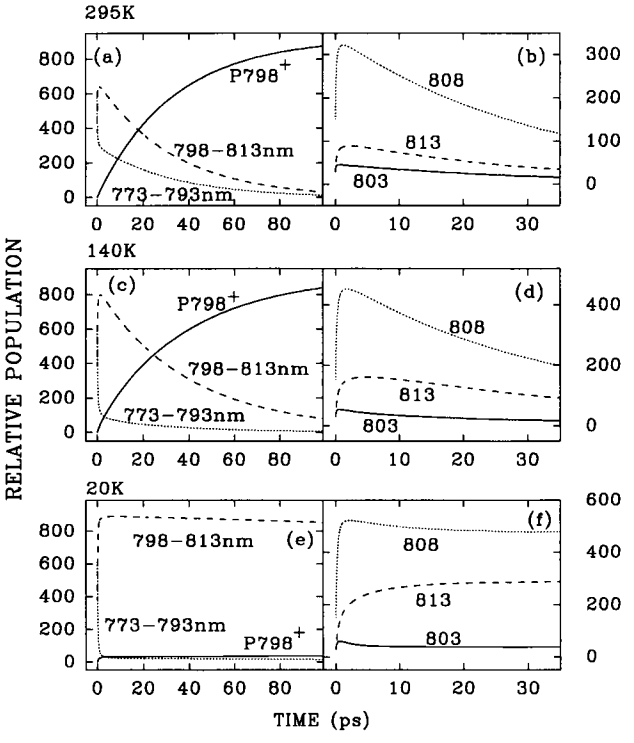

FIGURE 7 Kinetic traces calculated from the random model. The layout is the same as in Fig. 6.

DISCUSSION

Spectral antenna heterogeneity

The results presented in this paper clearly illustrate that the antenna system of heliobacteria is spectrally heterogeneous. Several previous studies have indicated the presence of many spectral BChl *g* forms in the antenna of heliobacteria (Van Dorssen et al., 1985; Smit et al., 1989; Trost and Blankenship, 1989). Steady-state fluorescence measurements have indicated that all or nearly all fluorescence is emitted from the longest wavelength-absorbing form BChl *g* 808 at low temperature (Van Dorssen et al., 1985; Van Kan et al., 1989). A strong increase in the fluorescence yield was observed upon lowering the temperature (Van Dorssen et al., 1985), which was ascribed to a decrease in the overlap between the emission of the long wavelength antenna and the absorption of the primary donor in the reaction center (i.e., a decrease in the rate of energetically "uphill" excitation transfer). Time-resolved transient absorption measurements at low temperatures confirmed that excitations were transferred toward long wavelength antenna BChl *g* within a few picoseconds (Van Noort et al., 1994). These studies also revealed the presence of more than one spectral form within the so-called BChl *g* 808 pool. Long-lived (>50 ps) excited states were observed on pigments absorbing around 812–814 nm (Van Kan et al., 1990). Further evidence for multiple spectral forms within BChl *g* 808 came from time-resolved fluorescence measurements (Kleinherenbrink et al., 1993) and difference spectra caused by the formation of antenna triplets at low temperature (Smit et al., 1989; Kleinherenbrink et al., 1991).

The low temperature transient absorption measurements presented in this paper confirm that a number of spectral forms are present within the antenna of *Hc. mobilis* and provide information on kinetic processes within the antenna/reaction center complex. Evidence for spectral heterogeneity within the pool of BChl *g* 808 pigments is clearly obtained at 20 K, where an antenna bleaching remained around 814 nm after 170 ps (Figs. 3–5, see below). Furthermore, a clear energy transfer process with a time constant of 15 ps within the BChl *g* 808 pool was observed (Fig. 5). It may be noted that a precise assignment of the observed bleaching to excited states on pigments absorbing at specific wavelengths is complicated, because of an unknown contribution by stimulated emission to the spectra.

Rates of energy transfer within the antenna

Upon (sub)picosecond flash excitation of membranes of heliobacteria at room temperature, antenna excitations were found mostly to localize on the two longest wavelength

absorbing forms BChl *g* 793 and BChl *g* 808 within 1–2 ps (Van Noort et al., 1992; Lin et al., 1994). Antenna de-excitation and subsequent charge separation occurred in 20–30 ps, presumably by the so-called trapping-limited mechanism. The assumption of trapping limited kinetics is that all single excitation transfer steps are substantially faster than the charge separation in the reaction center (Pearlstein, 1984), for which a time of 1.2 ps was estimated (Lin et al., 1994). The model simulations using 0.2–0.25 ps single step hopping time and a charge separation time of 1.0 ps reproduce the experimental observations very well. A 1.0 ps spectral equilibration time among the antenna molecules and a 30 ps de-excitation time of the antenna were found using both the funnel model and random model simulations, in good agreement with the experimental results.

At low temperature, the energy differences between the spectrally separated pigments in the antenna and reaction center of heliobacteria are expected to substantially slow down at least some of the excitation transfer steps, and the trapping-limited model may no longer apply. Energy transfer from the bulk of antenna BChl *g* (absorbing below 800 nm) to the long wavelength forms was observed to occur within 1 ps, both at 140 and at 20 K (Figs. 2 and 5), which still reflects a sub-picosecond single-step hopping time (Figs. 6 and 7). After this fast equilibration process, the antenna excitations decay to form the charge-separated state in the reaction center with time constants of about 30 and 70 ps at 140 and 20 K, respectively (Figs. 2 and 5, see below). At 20 K, an additional process is observed with a time constant of 15 ps (Fig. 5), clearly reflecting a slower energy transfer process from pigments absorbing around 805 nm to pigments absorbing at even longer wavelengths within the BChl *g* 808 band. The relatively slow rate of this energy transfer process (compared with that of the charge separation) indicates that the strictly trapping limited model that was proposed for the description of the kinetics at room temperature is indeed not appropriate at 20 K.

The observation of the relatively slow 15 ps energy transfer process within the antenna has important implications for the possible organization of the different spectral forms of BChl *g*. In the simulations, when antenna molecules from different spectral forms were organized according to the "funnel" model arrangement, energy transfer toward the longest wavelength-absorbing pigments was unidirectional and fast at low temperatures. Such an antenna arrangement results in a fast equilibration, i.e., excitations concentrated on the long wavelength pigments and after that, the only energy transfer pathway is to the trap. The observed slow energy transfer process at 20 K (the 15 ps component in Fig. 5 *a*) implies that some of the pigments within the BChl *g* 808 band are surrounded in the antenna by pigments absorbing at shorter wavelengths. Such an arrangement would hinder energy transfer to pigments absorbing at even longer wavelengths and result in the observed slow transfer process.

The simulations using the "random" model results in such multiphasic kinetics at low temperatures (Fig. 7, *d* and *f*). A similar kinetic behavior of antenna excitations at low temperature was predicted from model calculations on the Photosystem I antenna, using a distribution of spectral forms (Jia et al., 1992; Trinkunas and Holzwarth, 1994). A slow energy transfer process was not observed in the kinetics of antenna excitations at 140 K (Fig. 2). This may be because of the technical difficulty of separating its kinetics from the overall antenna decay (because of trapping in the reaction center) with a time constant of 30 ps. The low amplitude of this component and the substantial spectral overlap at higher temperature may also contribute. However, especially at room temperature, it is more likely to be because of the effect of higher temperatures, which prevents isolated low energy pigments from acting as intermediate excitation traps.

Further evidence for the distribution of antenna pigments is found in the residual bleaching around 814 nm that remains in the difference spectrum at 20 K after 170 ps (Figs. 3–5). This bleaching does not appear in difference spectra of $P798^+$ formation at low temperature (Kleinherenbrink et al., 1991). It may be ascribed, therefore, to long-lived excitations on long wavelength-absorbing antenna pigments that are inefficient in energy transfer to the primary electron donor in the reaction center. If these pigments were all nearest neighbors to the reaction center, as predicted by the funnel model, all excitations should reach the primary electron donor through them, which is clearly not the case. A similar conclusion was recently reached by Van Noort et al. (1994), who assigned a long-lived excitation to BChl *g* pigments that were isolated, either spatially or energetically.

Overall excitation decay under high excitation intensities

In our experiments at high excitation intensity (Figs. 2 *b* and 5 *b*), about 0.9 photons were absorbed per reaction center, resulting in a maximum fraction of 45% of the reaction centers in the "closed" state (see Materials and Methods). There is a clear difference in the excited-state kinetics under high and low excitation intensities. Both at 140 and at 20 K, an additional component with a time constant of 6–7 ps is needed to fit the data using high excitation intensities, reflecting a bleaching decay at all wavelengths (compare Fig.2, *a* and *b* with Fig. 5, *a* and *b*).

The oxidized primary donor $P798^+$ has been shown to be a more efficient quencher of the steady-state fluorescence than P798 in the neutral state, especially at low temperatures (Deinum et al., 1991). Picosecond transient absorption measurements at 15 K in the presence of oxidized P798 revealed an excitation decay component with a time constant of 4 ps, which was assigned to quenching by $P798^+$ (Van Noort et al., 1994). Because the difference in the fraction of closed reaction centers at high and low excitation intensities is relatively small in our measurements, the 6–7 ps component observed under high intensity excitation must mainly be ascribed to excitation annihilation with a possible small contribution caused by quenching by $P798^+$. This annihilation is probably primarily singlet-singlet rather than singlet-triplet, because the lifetime of the triplet states of both P798

and the antenna pigments is about 350 μs in the closely related organism *Heliobacterium chlorum* (Smit et al., 1989). With this lifetime only about 0.5% of any triplets that form will remain at the time of the next flash 1.85 ms later.

The time constants and decay-associated spectra associated with the overall trapping of excitations (30 and 70 ps components in Figs. 2 and 5) and formation of the charge separated state (nondecaying spectra in Figs. 2 and 5) are similar at all excitation intensities used. This indicates that after the annihilation processes have occurred, and only one excitation per reaction center remains, trapping of excitations proceeds in the same way as under low intensity excitation. In our experiments with low excitation intensities (Figs. 2 *a* and 5 *a*), about 0.25 photons were absorbed per reaction per flash (see Materials and Methods), indicating that excitation annihilation effects may be largely neglected. With a lifetime of the oxidized primary donor at low temperature of about 2.3 ms (Smit et al., 1985), it can be estimated that only 11% of the reaction centers are kept in the "closed" state (P798 oxidized) by the excitation flashes at 540 Hz (see Materials and Methods). This calculation assumed that every absorbed photon results in a charge-separated state, which is probably not true at 20 K, so the actual amount of oxidized P798 is probably somewhat less than 11% under these conditions.

Efficiency of photochemistry at low temperature

An important question that arises at low temperature is whether "uphill" energy transfer from long wavelength antenna pigments to the primary electron donor in the reaction center still occurs. The yield of photochemistry upon excitation of BChl *g* was found to be 70% at 6 K (Van Dorssen et al., 1985; Kleinherenbrink et al., 1992), so it is clear that at least most of the excitations are eventually trapped even at low temperatures. The process of energy transfer to the reaction center has not been time-resolved at low temperature before the present work. Unfortunately, it is difficult to estimate quantitatively the yield of charge-separated states from experiments of the sort reported in this paper, because of uncertainties in relative extinction coefficients of the various pigments and the possibility of at least partial buildup of charge-separated states, as discussed above.

The experimental results presented in this paper clearly demonstrate energy transfer from long wavelength antenna pigments to the primary electron donor P798 in the reaction center and subsequent formation of the charge-separated state at temperatures as low as 20 K. The time constant for this process was 30 ps at 140 K and 70 ps at 20 K. The temperature dependence of this process (a time constant of 20–30 ps) was obtained at room temperature (Van Noort et al., 1992; Lin et al., 1994) appears to be surprisingly weak.

Limitations of the simulations

Simulations of energy transfer and trapping in photosynthetic antenna systems are at a very low level of sophistication, primarily because of the lack of high resolution structural information. These structural data are essential to predict accurately energy transfer pathways and rates. Lattice models, in which the pigments are arranged on a periodic lattice, although very useful in many ways, can never recover the details of the pigment orientations and interactions that ultimately are essential in determining how the actual system behaves. The most critical interaction, the one between the photoactive pigments and the spatially nearest antenna pigments, is also the least well understood. The use of more accurate lineshape functions and three-dimensional lattices are an improvement but do not really solve the most critical problem, which is the lack of accurate structural information. Thus, although the current simulations are useful to rule out certain idealized arrangements of pigments, such as the funnel model discussed above, they cannot be expected to reproduce accurately the details of energy transfer and trapping, especially at low temperature.

The random model simulations at 20 K reproduce the observed relaxation processes within the antenna pigments reasonably well, as discussed above. However, the simulations do a poor job of predicting efficient charge separation at low temperatures. To obtain a reasonably high yield of $P798^+$ in the simulations, either the trapping time τ_{trap} (uphill transfer from antenna to reaction center) has to be made an unreasonable 10^{-8} ps or the energy level of the reaction center has to be lowered to approximately 808 nm. The latter implies that the energy level of the trap (around 808 nm) is at a significantly lower energy than the P798 bleaching at 20 K. The most straightforward remedy for this apparent discrepancy would be to assume a much smaller difference between the (0–0) energies of the primary electron donor P798 and the long wavelength antenna. Because information about the Stokes shift of P798 and antenna BChl *g* is lacking, this conclusion cannot be verified at present. However, there are indications that the Stokes shift of the antenna pigments of several species are considerably smaller than those of the respective primary donor (Trissl, 1993). Studies of isolated reaction centers of purple bacteria have shown that the 0–0 transition band of the special pair is at a much longer wavelength than that of the bleaching maximum of the special pair. A 15 nm difference is found in *Rhodobacter sphaeroides* and 25 nm for *Rhodopseudomonas viridis* (Trissl, 1993). Because the 0–0 energy for P798 in the reaction center of heliobacteria is not accurately known, the energy level of the trap used in the simulation could introduce a large error. Similar problems were also found in simulations on Photosystem I (Jia et al., 1992; Trinkunas and Holzwarth, 1994).

Thus, although both steady-sate and time-resolved experimental measurements indicate that charge separation indeed takes place at low temperatures with a relatively high quantum yield, the simulations done so far do not adequately reproduce this result. The excitations localize in the low energy antenna pigments and never escape. Low temperature simulations of Photosystem I trapping suffer the same problem (Jia et al., 1992; Trinkunas and Holzwarth, 1994). This problem represents a significant gap in our understanding of the function of photosynthetic antennas.

Several reasons can be considered for the larger discrepancy of simulations at low temperatures compared with room temperature. These points have also been considered in recent simulations of Photosystem I (Trinkunas and Holzwarth, 1994; Laible et al., 1994). First, the approximation using a two-dimensional regular lattice model might not be able to provide enough interactions among antenna molecules as well as between antenna and the trap. Including next-nearest neighbor interaction made a significant contribution to the simulated energy transfer processes at low temperature. It is likely that a quasi-three-dimensional model would improve the predicted energy transfer efficiency to the trap, although a detailed structure is necessary before this can be accurately assessed, as discussed above. The second reason is the approximation of using Boltzmann factors to calculate the back transfer rate. Because the knowledge of the temperature dependence of the line shape change of absorption and emission for each spectral forms is lacking, as well as the orientation of each antenna molecule, an accurate Förster transfer rate cannot be calculated. Using the Boltzmann factor to calculate the back transfer rate depends on the number of spectral forms used and the band position of each spectral form. Better simulations were obtained at low temperatures when more spectral forms were used in the simulation. The third reason is the energy level of the trap used, as discussed above.

Despite the approximations used in the simulation, the results give useful information about the role of each spectral form in the energy transfer and trapping processes and the possible antenna arrangement in such a simple photosynthetic system. It also provides an indication of how the microscopic time constants relate to the observed kinetic constants. The microscopic constants that work well in our simulations, such as the single-step transfer time and the charge separation time, agree well with values estimated from previous work in similar systems (e.g., Owens et al., 1989; Jia et al., 1992; Trinkunas and Holzwarth, 1994; Laible et al., 1994).

CONCLUSIONS

Detailed transient absorption measurements of excitation transfer in the spectrally heterogeneous antenna-reaction center complex of *Hc. mobilis* at low temperatures were taken. Excitation transfer to long wavelength-absorbing antenna BChl *g* was observed to occur within about 1 ps. Furthermore, a considerably slower excitation redistribution process was observed within the long wavelength-absorbing BChl *g* pool at 20 K. Energy transfer from long wavelength antenna pigments to the primary electron donor P798 in the reaction center was observed for the first time at low temperatures. Simulations using both a funnel model and a random model result in kinetics similar to the experimental results at room temperature and at 140 K. The simulations give a sub-picosecond single-step transfer time and a charge separation time of 1 ps at room temperature. The 15 ps phase of excitation equilibration at 20 K could best be described in terms of the random model. Neither model adequately described the trapping process at 20 K. The relatively small number of antenna BChls associated with the reaction center in the membrane of heliobacteria and the availability of detailed measurements of energy transfer processes at low temperature make these systems a very suitable subject of kinetic model studies, similar to those performed for the related but more complicated Photosystem I.

We thank Dr. G. Hastings for helpful discussions.
Funding for this research was from National Science Foundation grant DMB-9106685. This is publication #211 from the Arizona State University Center for the Study of Early Events in Photosynthesis.

REFERENCES

Beauregard, M., I. Martin, and A. R. Holzwarth. 1991. Kinetic modeling of exciton migration in photosynthetic systems. I. Effects of pigment heterogeneity and antenna topography on exciton kinetics and charge separation yields. *Biochim. Biophys. Acta.* 1060:271–283.

Blankenship, R. E., D. C. Brune, and B. P. Wittmershaus. 1988. Chlorosome antennas in green photosynthetic bacteria. *In* Light-Energy Transduction in Photosynthesis: Higher Plants and Bacterial Models. S. E. Stevens, Jr. and D. Bryant, editors. American Society of Plant Physiologists, Rockville, MD. 32–46.

Brune, D. C., T. Nozawa, and R. E. Blankenship. 1987. Antenna organization in green photosynthetic bacteria I. Oligomeric bacteriochlorophyll *c* as a model for the 740 nm absorbing bacteriochlorophyll *c* in *Chloroflexus aurantiacus* chlorosomes. *Biochemistry.* 26:8644–8652.

Cho, F., and Govindjee. 1970. Low temperature (4–77 K) spectroscopy of *Anacystis*: temperature dependence of energy transfer efficiency. *Biochim. Biophys. Acta.* 216:151–161.

Clayton, R. K., and B. J. Clayton. 1972. Relations between pigments and proteins in the photosynthetic membranes of *Rhodopseudomonas spheroides. Biochim. Biophys. Acta.* 283:492–504.

Deinum, G., H. Kramer, T. J. Aartsma, F. A. M. Kleinherenbrink, and J. Amesz. 1991. Fluorescence quenching in *Heliobacterium chlorum* by reaction center in the charge separated state. *Biochim. Biophys. Acta.* 1058:339–344.

Förster, Th. 1965. Delocalized excitation and excitation transfer. *In* Modern Quantum Chemistry, Vol. III. O. Sinanoglu, editor. Academic Press, New York. 93–137.

Golbeck, J. H. 1992. Structure and function of Photosystem I. *Annu. Rev. Plant Physiol. Plant Mol. Biol.* 43:293–324.

Hastings, G., F. A. M. Kleinherenbrink, S. Lin, and R. E. Blankenship. 1994. Time-resolved fluorescence and absorption spectroscopy of Photosystem I. *Biochemistry.* 33:3185–3192.

Holzwarth, A. R., G. Schatz, H. Brock, and E. Bittersmann. 1993. Energy transfer and charge separation kinetics in Photosystem-I. 1. picosecond transient absorption and fluorescence study of cyanobacterial Photosystem-I particles. *Biophys. J.* 64:1813–1826.

Hunter, C. N., and R. Van Grondelle. 1988. The use of mutants to investigate the organization of the photosynthetic apparatus of *Rhodobacter sphaeroides. In* Photosynthetic Light-Harvesting Systems: Organization and Function. H. Scheer and S. Schneider, editors. Walter de Gruyter & Co., Berlin. 247–260.

Jia, Y., J. M. Jean, M. M. Werst, C.-K. Chan, and G. R. Fleming. 1992. Simulations of the temperature dependence of energy transfer in the PS I core antenna. *Biophys. J.* 63:259–273.

Kirmaier, C., and D. Holten. 1990. Evidence that a distribution of bacterial reaction centers underlies the temperature and detection-wavelength dependence of the rates of the primary electron-transfer reactions. *Proc. Natl. Acad. Sci. USA.* 87:3552–3556.

Kleinherenbrink, F. A. M., T. J. Aartsma, and J. Amesz. 1991. Charge separation and formation of bacteriochlorophyll triplets in *Heliobacterium chlorum. Biochim. Biophys. Acta.* 1057:346–352.

Kleinherenbrink, F. A. M., P. Cheng, J. Amesz, and R. E. Blankenship. 1993. Lifetimes of bacteriochlorophyll fluorescence in *Rhodopseudomo-*

nas viridis and *Heliobacterium chlorum* at low temperatures. *Photochem. Photobiol.* 57:13–18.

Kleinherenbrink, F. A. M., G. Deinum, S. C. M. Otte, A. J. Hoff, and J. Amesz. 1992. Energy transfer from long-wavelength absorbing antenna bacteriochlorophylls to the reaction center. *Biochim. Biophys. Acta.* 1099:175–181.

Kramer, H. J. M., J. D. Pennoyer, R. Van Grondelle, W. M. J. Westerhuis, R. A. Niederman, and J. Amesz. 1984. Low-temperature optical properties and pigment organization of the B875 light-harvesting bacteriochlorophyll-protein complex of purple photosynthetic bacteria. *Biochim. Biophys. Acta.* 767:335–344.

Laible, P. D., W. Zipfel, and T. G. Owens. 1994. Excited state dynamics in chlorophyll-based antennae: the role of transfer equilibrium. *Biophys. J.* 66:844–860.

Lin, S., H.-C. Chiou, F. A. M. Kleinherenbrink, and R. E. Blankenship. 1994. Time-resolved spectroscopy of energy transfer and electron transfer processes in the photosynthetic bacterium *Heliobacillus mobilis. Biophys. J.* 66:437–445.

Nuijs, A. M., R. J. Van Dorssen, L. N. M. Duysens, and J. Amesz. 1985. Excited states and primary photochemical reactions in the photosynthetic bacterium *Heliobacterium chlorum. Proc. Natl. Acad. Sci. USA.* 82: 6865–6868.

Olson, J. M. 1980. Chlorophyll organization in green photosynthetic bacteria. *Biochim. Biophys. Acta.* 594:33–51.

Owens, T. G., S. P. Webb, L. Mets, R. S. Alberte, and G. R. Fleming. 1989. Antenna structure and excitation dynamics in Photosystem I. II. Studied with mutants of *Chlamydomonas reinhardtii* lacking Photosystem II. *Biophys. J.* 56:95–106.

Smit, H. W. J., R. J. Van Dorssen, and J. Amesz. 1989. Charge separation and trapping efficiency in membranes of *Heliobacterium chlorum* at low temperature. *Biochim. Biophys. Acta.* 793:212–219.

Trinkunas, G., and A. R. Holzwarth. 1994. Kinetic modeling of exciton migration in photosynthetic systems. 2. Simulations of excitation dynamics in two-dimensional photosystem I core antenna/reaction center complexes. *Biophys. J.* 66:415–429.

Trissl, H.-W. 1993. Long-wavelength absorbing antenna pigments and heterogeneous absorption bands concentrate excitons and increase absorption cross section. *Photosynth. Res.* 35:247–263.

Trost, J. T., and R. E. Blankenship. 1989. Isolation of a photoactive photosynthetic reaction center-core antenna complex from *Heliobacillus mobilis. Biochemistry.* 28:9898–9904.

Turconi, S., G. Schweitzer, and A. R. Holzwarth. 1993. Temperature dependence of picosecond fluorescence kinetics of a cyanobacterial photosystem I particle. *Photochem. Photobiol.* 57:113–119.

Van de Meent, E. J., F. A. M. Kleinherenbrink, and J. Amesz. 1990. Purification and properties of an antenna-reaction center complex from heliobacteria. *Biochim. Biophys. Acta.* 1015:223–230.

Van Dorssen, R. J., H. Vasmel, and J. Amesz. 1985. Antenna organization and energy transfer in membranes of *Heliobacterium chlorum. Biochim. Biophys. Acta.* 809:199–203.

Van Dorssen, R. J., C. N. Hunter, R. Van Grondelle, A. H. Korenhof, and J. Amesz. 1988. Spectroscopic properties of antenna complexes of *Rhodobacter sphaeroides in vivo. Biochim. Biophys. Acta.* 932: 179–188.

Van Grondelle, R., H. Bergstrom, V. Sundstrom, R. J. Van Dorssen, M. Vos, and C. N. Hunter. 1988. Excitation energy transfer in the light-harvesting antenna of photosynthetic purple bacteria: the role of the long-wavelength absorbing pigment B896. *In* Photosynthetic light-harvesting systems: Organization and function. H. Scheer and S. Schneider, editors. Walter de Gruyter, Berlin. 520–530.

Van Kan, P. J. M., T. J. Aartsma, and J. Amesz. 1990. Excitation transfer and charge separation in *Heliobacterium chlorum* at 15 K. *In* Current Research in Photosynthesis, Vol. II. M. Baltscheffsky, editor. Kluwer, Dordrecht. 185–188.

Van Mourik, F., K. J. Visscher, J. M. Mulder, and R. Van Grondelle. 1993. Spectral inhomogeneity of the light-harvesting antenna of *Rhodospirillum rubrum* probed by T-S spectroscopy and singlet triplet annihilation at low temperatures. *Photochem. Photobiol.* 57:19–23.

Van Noort, P. I., T. J. Aartsma, and J. Amesz. 1994. Energy transfer and trapping of excitations in membranes of *Heliobacterium chlorum* at 15 K. *Biochim. Biophys. Acta.* 1184:21–27.

Van Noort, P. I., D. A. Gormin, T. J. Aartsma, J. Amesz. 1992. Energy transfer and primary charge separation in *Heliobacterium chlorum* studied by picosecond time-resolved transient absorption spectroscopy. *Biochim. Biophys. Acta.* 1140:15–21.

Werst, M., Y. Jia, L. Mets, and G. R. Fleming. 1992. Energy transfer and trapping in the photosystem I core antenna: a temperature study. *Biophys. J.* 61:868–878.

Wittmershaus, B. P., V. M. Woolf, and W. F. J. Vermaas. 1992. Temperature dependence and polarization of fluorescence from photosystem I in the *cyanobacterium Synechocystis* PCC 6803. *Photosynth. Res.* 31:75–87.

Woolf, V. M., B. P. Wittmershaus, W. F. J. Vermaas, and T. D. Tran. 1994. Resolution of low-energy chlorophylls in Photosystem I of *Synechocystis* sp. PCC 6803 at 77 and 295 K through fluorescence excitation anisotropy. *Photosynth. Res.* 40:21–34.